Chapter 1
Gold Nanostar Synthesis and Functionalization with Organic Molecules

Piersandro Pallavicini, Elisa Cabrini, and Mykola Borzenkov

Abstract This chapter is devoted to the synthesis and functionalization of gold nanostars. The physical-chemical characterization and singular features of gold nanostars with respect to other types of gold nanoparticles are provided. Various methods of GNS synthesis as well as of the functionalization of GNS with PEG, organic dyes, and bioactive compounds are discussed.

Keywords Gold nanostars • Seeded growth process • PEGylation • Fluorescence • Bioactive molecules

Before starting the review, Table 1.1 summarizes the information collected in this chapter.

1.1 Gold Nanoparticle Synthesis: Brief Introduction

A brief survey of the general techniques of GNP synthesis is required before we can analyze the different approaches to the gold nanostar synthesis.

The chemical reduction of transition metal salts in the presence of stabilizing agents with the subsequent generation of zerovalent metal colloids in aqueous or organic media is one of the most common and powerful synthetic methods in this field [1]. The simplest and by far the most commonly used protocol for the preparation of gold nanoparticles is the aqueous reduction of gold salt by sodium citrate at reflux [1, 2]. Generally, GNPs are synthesized in a liquid by reduction of chloroauric acid ($HAuCl_4$). During this process Au^{3+} ions are reduced to neutral gold atoms, the solution becomes supersaturated, and gold gradually starts to precipitate in the

P. Pallavicini • E. Cabrini
Department of Chemistry, University of Pavia, Viale Taramelli 12, Pavia 27100, Italy

M. Borzenkov (✉)
Department of Physics, University of Milano-Bicocca, Piazza Della Scienza 3, Milan 20216, Italy
e-mail: mykola.borzenkov@unimib.it

G. Chirico et al., *Gold Nanostars*, SpringerBriefs in Materials,
DOI 10.1007/978-3-319-20768-1_1

Table 1.1 Synthesis and functionalization of gold nanostars (summary of this chapter)

Synthesis of GNS	• In situ methods • Seed growth methods • Non-"seed-mediated" method • One-pot methods • Electron beam lithography technique
Functionalization of GNS	• PEGylation of GNS • Functionalization with dyes • Functionalization with DNA, proteins, aptamers, etc.

form of sub-nanometer particles [1, 3]. In general, the preparation process of GNP by chemical reduction contains two steps: (1) reduction using agents such as borohydrides, aminoboranes, hydrazine, formaldehyde, hydroxylamine, saturated and unsaturated alcohols, citric and oxalic acids, polyols, sugars, hydrogen peroxide, sulfites, carbon monoxide, hydrogen, acetylene, and monoelectronic reducing agents including electron-rich transition-metal sandwich complexes, and (2) stabilization by agents such as trisodium citrate dihydrate, sulfur ligands (in particular thiolates), phosphorus ligands, nitrogen-based ligands (including heterocycles), oxygen-based ligands, dendrimers, polymers, and surfactants [4]. The particle size depends on a large number of parameters; for example it can be controlled by the initial reagent concentrations [1, 3].

The preparation of GNP by reduction of $HAuCl_4$ and citrate-stabilized gold nanoparticles has been regarded as the most popular one for a long time, since their introduction by Turkevich [5]. The $HAuCl_4$ solution is boiled, and the trisodium citrate dihydrate is then quickly added under vigorous stirring. After a few minutes, the wine-red colloidal suspension is obtained, and the GNP size is about 20 nm [4, 5]. This technique was improved later by Frens, who obtained a broad size range of gold nanoparticles (from 15 to 150 nm) by controlling the trisodium citrate to Au ratio [2]. Nowadays the "in situ" Turkevich-Frens method has been further improved for reproducible preparation of citrate-stabilized gold nanoparticles [6–9].

The two-phase Brust-Schiffrin method, published in 1994, was the first method that allows to prepare the thiolate-stabilized gold nanoparticles via in situ synthesis using $NaBH_4$ as reduction agent, since it met great success [4, 10]. This method is performed in ambient conditions with relative high stability of the resulting GNPs. This method is suitable for obtaining particles in organic solvents. The GNPs are stabilized by relatively strong Au-S bonds and their diameters are in the 2–5 nm range, with the size much smaller than that of Turkevich [4]. Later this technique was improved by various research groups introducing thiolate-liganded gold nanoparticles [11–13].

The seed growth method is another popular technique for GNP synthesis. Compared with the in situ synthesis, the seed growth method enlarges the particles step by step, and it is easier to control the sizes and shapes of resulted gold nanoparticles. Therefore, this method is widely used in the most recent size- and shape-controlled GNP syntheses. Generally this process involves two steps. In the first step, small-size

AuNP seeds are prepared. In the second step, the seeds are added to a "growth" solution containing $HAuCl_4$ and the stabilizing and reducing agents. The newly reduced Au^0 grows on the seed surface starting from small gold crystals to form then large-size AuNPs. The reducing agents used in the second step are always mild ones that reduce Au^{3+} to Au^0 only in the presence of Au seeds as catalysts; thus the newly reduced Au^0 can only assemble on the surface of the Au seeds, and no new particle nucleation occurs in solution [4]. The initial procedures of preparation of GNP by seed growth were modified by El-Sayed using hexadecyltrimethylammonium bromide (CTAB) as the stabilizer instead of citrate [14]. These Au seeds with a diameter smaller than 4 nm were used to promote the narrow dispersity of GNP. GNPs with various shapes have been synthesized using the seed growth method [14].

1.2 Synthesis of Gold Nanostars

1.2.1 General Characterization of Gold Nanostars

As it has been already mentioned the optical properties of gold nanoparticles are of the great importance for application in various fields, especially for biomedical purposes. For anisotropic GNP it has been demonstrated that the presence of sharp edges and tips provides a very high sensitivity to local changes in the dielectric environment, as well as larger enhancements of the electric fields around the nanoparticles [15]. These features constitute the basis of LSPR- and surface enhancement Raman scattering (SERS)-based detections [16]. Hence, besides the main synthetic techniques described previously, an increasing number of synthetic routes are being developed, aiming at a simultaneous control of the size and shape of gold nanoparticles. Therefore, nonspherical gold nanoparticle synthesis has been the subject of numerous publications recently.

Among the various types, gold nanostars and in general multibranched gold nanoparticles have received much attention [17, 18]. Star-shaped GNPs have plasmon bands that are tunable into the NIR region, and the structure contains multiple sharp branches that act as "lightning rods" to greatly enhance the local EM field. The fabrication of gold nanostars has been driven by the interest on the LSPR response to the environment. This is particularly connected to GNS that display sharp tips and edges, where light can be highly concentrated [18, 19], and their structure is shown in Scheme 1.1. GNS colloids display two wide but distinct LSPR features including an intense band typically centered around 650–900 nm and a weaker band/shoulder located at ca. 500–600 nm [18]. When laser irradiated at the wavelength of their NIR band, GNS exhibit excellent transduction of absorbed light into heat [20]. Therefore, these types of gold nanoparticles could serve as effective tools for nanomedicine application. Moreover, nanostars display stronger SERS activity than spheres or even rods [21].

The following subchapter is devoted to the overview of different strategies of synthesis of different types of multibranched gold nanoparticles (see Scheme 1.1).

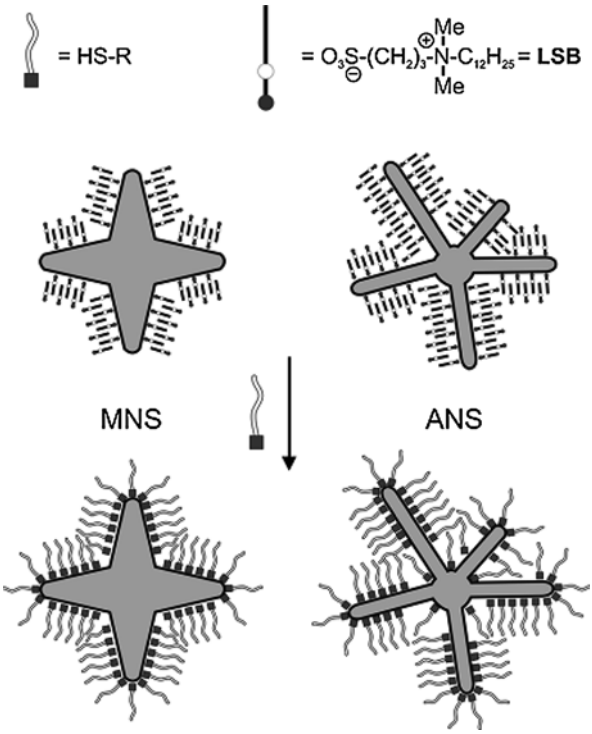

Scheme 1.1 The schematic structures of monocrystalline GNS (MNS) and penta-twinned asymmetric GNS (ANS) obtained by seed growth method assisted by the LSB surfactant. Protective surfactant and thiolated layers are also shown (reproduced from Casu et al. [17])

1.2.2 Synthesis of Gold Nanostars: An Overview of Synthetic Strategies

A wide variety of synthetic methods is available for the preparation of anisotropic gold nanoparticles with narrow size and shape distribution, and with specific branching degree. The choice of one or another of these preparative methods for star-shaped GNP depends on a number of relevant experimental parameters that determine the nucleation and growth steps of the particle synthesis, providing fine control over size and degree of branching of the nanoparticles [18, 22]. Both in situ and seed growth methods have been proposed during last 10 years for the synthesis of GNS. A recent review by Liz-Marzan et al. summarizes various synthetic approaches, optical properties, and application of GNS [18].

The most common method of GNS synthesis adopts seeded growth process, also widely employed for the synthesis of gold nanorods [14]. This process involves the reduction of chloroauric acid with ascorbic acid at ambient temperature on pre-synthesized gold nanoseeds and in the presence of surfactants (in most cases CTAB) [18, 23, 24]. These capping agents (surfactants or polymers) have preferential adsorption on certain crystalline facets of the metal seeds and have been claimed to trigger

the anisotropic growth process, through alteration of the growth rates along specific crystallographic directions [25]. It was shown for example that addition of $AgNO_3$ at different stages of nanocrystal growth increases the degree of control of the shape for penta-twinned gold nanoparticles [26]: penta-branched gold nanocrystals were obtained with sizes ranging from 70 to 350 nm and comprising single-crystalline tips with {111} outer faces. This study allowed not only to control the final nanostar morphology, but also to increase dramatically the yield of branched particles. In 2004 Murphy and coworkers studied the influence bromide ions by replacing CTAB with its chloride equivalent (CTAC) and adding different amounts of NaBr to achieve a better control over bromide concentration [24].

The nature of reducing agent was also studied. For example, in the paper published in 2006 in *Nanotechnology*, hydroxylamine sulfate was used in the preparation of polycrystalline-branched gold nanoparticles with sizes ranging from 47 nm up to 185 nm in a stepwise growth approach [27]. It has been reported that highly branched nanoparticles can be obtained upon addition of $HAuCl_4$ in the presence of 15 nm poly(vinylpyrrolidone) (PVP)-coated gold seeds, when the concentration of PVP in solution is high [28]. This process can be performed at room temperature in very short time. It was also observed that no significant changes in size and shape of nanostars were induced by changing the molecular weight of PVP. A simple one-step synthesis protocol for stable gold nanostars was recently reported [29], based on the reduction of a gold precursor in a basic environment using hydroxylamine as a reducing agent. These star-shaped gold nanostructures showed a higher amplification of the Raman scattering of rhodamine 6G molecules relative to spherical nanoparticles of the same dimension.

Khoury and Vo-Dinh reported in 2008 the controlled synthesis of high-yield gold nanostars ranging from 45 to 116 nm [30]. GNS were synthesized by extending the protocol reported by Liz-Marzan et al. [15], in order to enable size control of the stars from approximately 45 to 116 nm in size. This size range translates to tuning capabilities of the longitudinal plasmon peak in the NIR region from around 725 to over 850 nm. The authors used 20 nm PVP-coated gold seeds in ethanol and investigated the growth of GNS as a function of time during the synthesis by monitoring the spectrum of the GNS suspension and by imaging stars' morphological changes over time via TEM. As it was stated previously most nanostar synthesis requires the use of a surfactant (e.g., CTAB or PVP). In the paper published in *Nanotechnology* in 2012 [31] Khoury and coworkers presented a new, surfactant-free synthesis method of biocompatible gold nanostars with adjustable geometry that allows to tune the plasmon band into the near-infrared (NIR) region "tissue diagnostic window," which is most suitable for in vivo imaging [31]. Nanostars were prepared by a seed-mediated growth method within 1 min in high yield without the use of the toxic surfactant. To obtain nanostars of similar sizes and concentrations but of different geometries, authors investigated multiple factors, including pH, stirring speed, and concentration ratios of $AgNO_3$, ascorbic acid, $HAuCl_4$, and seed. In general, nanostars synthesized under lower pH, moderate vortexing speed, and ascorbic acid/$HAuCl_4$ ratio of 1.5–2 produced the most red-shifted plasmon.

Osinkina et al. reported a two-step approach for the fabrication of quasi-hexagonal ordered arrays of star-shaped gold nanoparticles for SERS spectroscopy by a combination of block-copolymer micelle nanolithography and electroless deposition [32]. Arrays of single-gold nanoparticles were fabricated by block-copolymer micelle nanolithography. Gold nanostars were prepared by incubating the samples in an aqueous solution of CTAB, gold (III) chloride hydrate, ascorbic acid, and silver nitrate. In a second paper published in 2013, GNS with tunable morphology were synthesized by a seed-mediated growth method using poly(diallyldimethylammonium chloride) as stabilizer [33]. The number and length of the branches of the nanostars can be controlled by adjusting the amount of silver nitrate. In a similar approach Chirea in a paper published in *Catalysts* in 2013 described gold nanostars (≈70 nm tip-to-tip distance) synthesized by seed-mediated method and covalently self-assembled on 1,5-pentanedithiol-modified electrodes [34]. The average core diameters and tip length of the GNS were 50 and 19 nm. These gold nanostars displayed two surface plasmon bands: a dominant broad feature at the edge of the visible range (≈837 nm). The cores produce instead a surface plasmon band at 545 nm. Kereselidze et al. developed the synthesis protocol for 180–300 nm GNS by means of a silver-seed-mediated method [35, 36]. Highly multibranched gold nanostars were also obtained at room-temperature synthesis assisted by deep-eutectic solvents (DES). DES is an ionic solvent composed of a mixture of quaternary ammonium salts with hydrogen donors, which shows a melting point much lower than that of the individual components. The advantages of DES-mediated synthesis are the high viscosity, polarity, thermal stability, ease of preparation, and low cost of the products. In addition, DES forms a highly structured "supramolecular" solvent, because of the extended hydrogen-bond network in the liquid state. The concentration of the ascorbate ions and the presence of water in the solution were found to have a profound influence on the formation of branches [37]. Stassi et al. investigated the relationship between the particle diameter, the protuberance size and shape, and the easiest and cost-effective reaction conditions. The corresponding gold nanostars were prepared by mild reduction of $HAuCl_4 \cdot 3H_2O$ with L-ascorbic acid in the presence of DES, prepared from choline chloride and urea in a 1:2 mixture.

Interesting methods of GNS synthesis were developed by Pallavicini et al. By replacing CTAB with the zwitterionic lauryl sulfobetaine (LSB) surfactant in the classical seed growth synthesis, monocrystalline gold nanostars and penta-twinned gold asymmetric nanostars were obtained instead of nanorods [17]. The main product under all synthetic conditions was asymmetric nanostars, which have branches with high aspect ratios, thus leading to LSPR absorptions in the 750–1150 nm range. The position of their LSPR absorption can be tuned up simply by regulating the concentration of reductant, the concentration of surfactant, or the concentration of the "catalytic Ag^+" cation. A growth mechanism that involves the direct contact of the sulfate moiety of LSB on the surface of the nano-object was proposed, thereby implying preferential coating of the {111} Au faces with weak interactions. Another benefit of using LSB surfactant instead of CTAB is that CTAB is cytotoxic and strongly bound to GNP. Therefore, the removal or substitution of

CTAB from GNP surface could be tricky or incomplete. In the next paper of the same research group published in 2013 five-branched gold nanostars were obtained using nonionic Triton X-100 surfactant in a seed growth synthesis [38]. The synthesized nanoparticles have the uncommon feature of two intense localized LSPRs in the NIR range 600–900 and 1100–1600 nm, besides the common visible LSPR ranges. Au nanoseeds were generated from $AuCl_4$ by means of $NaBH_4$ in the solutions of high surfactant concentration (0.05–0.15 M). The absorption spectra of growth solutions obtained in 0.05 M Triton X-100 and TEM images of resulted GNS are shown in Scheme 1.2.

Nehl et al. described the fabrication of GNS by a modified seed-mediated, surfactant-directed synthesis based on reduction of gold chloride [39]. This method was modified by means of different seed particles or by increasing the growth rate.

Feldmann and coworkers reported instead a water-based, non-"seed-mediated" GNS synthesis [40] method with high yield. This method allows to change the number and size of the spikes and the overall size of the particles, and hence to tune

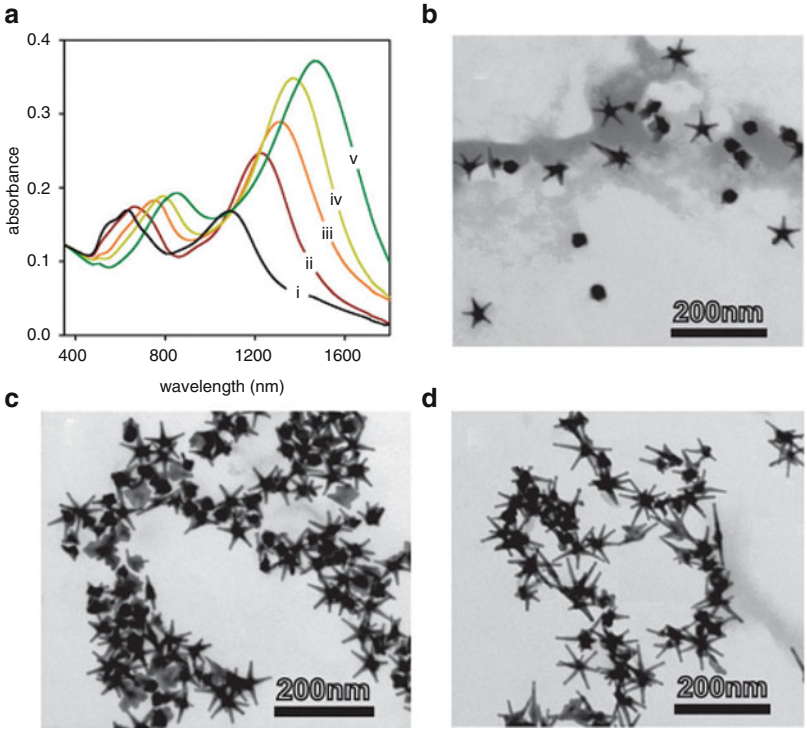

Scheme 1.2 (**a**) Absorption spectra of growth solutions obtained in 0.05 M od Triton X-100 and increasing concentration of ascorbic acid: (1) 1.576 10^{-3} M; (2) 1.773 10^{-3} M; (3) 2.364×10^{-3} M; (4) 2.758×10^{-3} M; (v) 3.152×10^{-3} M. (**b**) TEM image of GNS obtained from the solution of spectrum (1). (**c**) The same from the solution of spectrum (3). (**d**) The same from the solution of spectrum (5) (reproduced from Pallavicini et al. [38])

the localized surface plasmon resonances of the particles over the broad spectral range in the visible and NIR. CTAB was employed as the capping and growth-regulating agent.

One-pot methods of preparation of gold nanoparticles involve the direct preparation of the precursor solution in the presence of suitable reducing agents and surfactants at room temperature by means of a variety of reactant concentration and reaction times [18, 41]. Various one-pot syntheses to produce gold nanostars have been developed recently [15, 18]. These protocols are based on the use of the "green" chemical *N*-2-hydroxyethylpiperazine-*N*-2-ethanesulfonic acid used as reducing and stabilizing agent. Thus, three-dimensional branched nanocrystals with 1–8 tips as well as flower-like gold nanoparticles with twinned tips were obtained in high yield [42, 43]. Examples of one-pot method of preparation of GNS assisted by surfactants and capping agents were also reported: star-shaped gold nanoparticles were obtained by reduction with ascorbic acid in the presence of PVP [44]. However, in this case star-shaped nanoparticles (7 %) and tripod or regular triangular plates (4 %) were observed among a large amount of spherical particles (89 %) including distorted or aggregated ones. In a different approach polydisperse branched GNPs were obtained with high yield using hydrogen peroxide and sodium citrate as reducing agents in combination with bis(*p*-sulfonatophenyl) phenylphosphine dehydrate dipotassium as stabilizer [45]. Very recently Hegmann and coworkers described a simple one-pot silver-assisted synthesis of GNS that employs $AgNO_3$ and a mild reducing agent, ascorbic acid, in the presence of a lyotropic liquid crystal (LLC) template formed by Triton X-100 in water either in the hexagonal phase or the micellar phase [46]. The LLC template is found to assist in the formation of well-defined nanostars with long, twinned thorns and provides the necessary colloidal stability that prevents the final nanostars from irreversible aggregation. The length of the thorns on the nanostars can be tailored by controlling the Au/Ag ratio in the growth solution. By using aminosugars, a series of multipodal gold nanostructures has been obtained via a one-pot chemical reduction method in aqueous solution and at room temperature [47]. The size and shape of these nanoparticles were controlled either by adjusting the amount of reducing agent or by quenching the reaction at a given time.

Other alternative methods of preparation of GNS have been reported. Notably, an electrochemical method was implemented in a two-electrode cell in which the electrochemical reduction of $HAuCl_4$ was carried out in the presence of PVP and NaOH [48]. Basic values of pH were essential to produce branched gold nanoparticles. The shape control could also be achieved by using a template-directed synthesis, where the template comprised a three-dimensional porous lattice of uniform iron nanoparticles [49].

The fabrication of GNS arrays by means of electron beam lithography, in which the plasmon resonance energy can be tuned via the nanostar size from the visible into the NIR region, was also reported [50]. In a second publication of the same research group plasmonic nanostar-dimers, decoupled from the substrate, have been fabricated by combining electron-beam lithography and reactive-ion etching techniques [51]. The 3D architecture, the sharp tips of the nanostars, and the sub-10 nm gap size promote the formation of giant electric field in highly localized hot spots.

1.3 Functionalization and Coating Approaches of GNS

Gold nanoparticles are widely used as sensing, targeting, imaging, and delivery nanobioplatforms. For these applications, surface functionalization with suitable ligands is essential to ensure particle stability against aggregation and for targeting approaches [52, 53]. Various conjugation methods of gold nanoparticles with biomolecules have been developed for specific targeting, for drug delivery, and for sensing assays [53]. Finely tuned surface functionalization of the nanoparticles, which determines their interaction with the environment, is required [54]. These interactions ultimately affect the colloidal stability of the particles, and may yield to a controlled assembly or to the delivery of nanoparticles to a target. The surface of GNS can be functionalized similar to all other gold nanostructures. However, the high shape anisotropy adds specific features to their surface decoration. Thus, in this subchapter the functionalization approaches of GNS with various organic molecules are reviewed.

1.3.1 PEGylation of GNS

For various applications of gold nanoparticles, PEGylation is one of the most widely used functionalization strategies as it has numerous advantages. Polyethylene glycol (PEG) is known to reduce reticuloendothelial system uptake and increase circulation time versus uncoated counterparts, by reducing the nonspecific binding of proteins as well as their cytotoxicity [55]. PEGylation is now commonly used to coat different kinds of nanoparticles, in order to improve their stability under physiological conditions and biocompatibility [55]. PEG enhances in vitro stability of nanoparticles in saline buffers or culture media and it allows the coated nanoparticles to evade macrophage-mediated uptake and removal from systemic circulation in vivo [56]. PEG decoration is also advantageously employed for nanoparticle-specific functionalization, as many commercial PEGs carry α-function suitable for grafting on gold (typically a thiol) and remote ω-function (e.g., –OH, –COOH, $–NH_2$) that may be efficiently used for further chemical modification [57, 58].

A comprehensive study of PEGylated gold nanostars and PEGylated bipyramidal-like nanostructures was presented by Navarro et al. in 2012 [59]. The nanoparticles were prepared at high yield and their surface was covered with a biocompatible PEG polymer. The PEGylated gold nanoparticles were incubated with melanoma B16-F10 cells. Dark-field microscopy showed that the biocompatible gold nanoparticles were easily internalized and most of them localized within the cells. Jo et al. performed the PEGylation of GNS synthesized by seed growth with bifunctional *O*-[2-(3-mercaptopropionylamino)ethyl]-*O′*-methylpolyethylene glycol [60]. These PEGylated gold nanostars were further conjugated with aptamers for the targeting of prostate cancer cells. The PEGylation of GNS with (*O*-[2-(3-mercaptopropionylamino) ethyl]-*O′*-methylpolyethylene glycol for in vivo particle tracking and photothermal ablation was also reported [61].

Surface modification of gold nanostars by means of PEGs with terminated thiol group (PEG-SH) with different molecular weights prevents the aggregation of the nanoparticles, due to the amphiphilic characteristic of the polymer (it is soluble both in water and organic solvents) [62]. Pallavicini et al. coated the GNS synthesized in the presence of the LSB surfactant with PEG_{2000}-SH [17]. Upon coating the long and intermediate LSPR bands shifted to the red (10 nm and 5 nm, respectively) due to the substitution of LSB on GNS surface with PEG_{2000}-SH. These functionalized GNS have an exceptional stability in acidic and base media, PBS solution, and ISO-sensitest broth (a defined medium suitable for use in antimicrobial susceptibility). Noticeably, if not coated with PEG these nanoparticles aggregate both in PBS and ISO-sensitest broth media within a few minutes. Almost negligible variation of absorption intensity was observed if larger thiolated PEG is used. These PEGylated GNS can be stored either in water or organic solvents due to amphiphilic nature of PEG. During the storage in organic solvents the LSPR position of the long and intermediate band displays a red shift that correlates linearly with solvent refractive index. In a following paper by the same research group, GNS were prepared in the presence of surfactant Triton X-100 and were coated with PEG_{2000}-SH [37]. The just synthesized GNS were poorly stable and the addition of PEG_{2000}-SH at the end of the growth promoted the displacement of surfactant. The whole GNS surface was coated yielding the extremely stable PEGylated nanostars. They can be dried, handled as powder, and redissolved in water or solvents ranging from ethanol to toluene, with both LSPRs shifting to the red. Also these PEGylated GNS display a photothermal behavior on both the intermediate (NIR) and long (SWIR) LSPR.

Wang et al. reported a new therapeutic strategy using chlorin e6-PEG-functionalized gold nanostars (GNS-PEG-Ce6) to couple photodynamic therapy with plasmonic photothermal therapy under single continuous wave laser irradiation [63]. GNS were conjugated with thiol-PEG-amine through the Au-S bonds. The PEGylated GNS exhibited excellent dispersivity and stability in a range of solutions including ultrapure water, dimethylformamide, phosphate-buffered saline (PBS), and cell medium with serum. PEGylated GNS were easily purified by centrifugation and conjugated with Ce6 (a commonly used photosensitizer) by NHS-EDC reaction in DMF. For further conjugation of GNS with fluorescence probes for in vivo imaging, bifunctional SH-PEG-NH_2 was employed [64]. PEGylated gold nanostars have been tested as contrast agents for photoacoustic imaging of blood vessels in the brain [65]. Moreover, anticancer drugs (e.g., DOX) were loaded into PEG-coated gold nanostars. Systematic administration of DOX-loaded PEG-GNS followed by NIR irradiation showed greater antitumor activity in a xenograft model of breast cancer than free Dox, PEGylated GNS, or NIR laser alone [65].

1.3.2 Functionalization of GNS with Dyes

The modification of nanoparticles with various fluorescent dyes is widely used because of the potential use of these systems for photosensing, light harvesting, and biosensing applications [66–69]. The immobilization of dye molecules onto

nanoparticles induces dramatic changes in its optical properties for chemical and biological applications, including fluorescence quenching of small dye molecules on gold nanoparticles. This effect can be exploited, for example, for protein sensing approaches [70]. Complementary oligonucleotides for single-stranded DNA-linked metal nanoparticles or bar-coded metal nanowires and fluorescent-dye-doped nanoparticles have been developed for medical diagnostics and labeling.

The reason for this success is clear. Fluorescent organic dyes are widely used for the detection of nucleic acids, proteins, and saccharides [71, 72]. However, these dyes suffer from photobleaching and can only be detected through highly sensitive techniques. On the other hand, gold nanoparticles are not susceptible to photobleaching and their absorption and scattering cross sections are larger than those of conventional dyes. Numerous methods have been utilized for detecting GNPs such as colorimetric, scanometric, fluorescence, surface-enhanced Raman scattering and electrochemical techniques [73]. These unique aspects have permitted the development of novel GNP-based assays for molecular diagnostics which promise increased sensitivity and specificity, multiplexing capability, and short turnaround times [73]. But also the interactions between nanoparticles and organic dyes have gained considerable interest for biochemical assays because they provide additional parameters to modulate the quenching efficiency and the photostability over classical dye-quenching system. Gold is also particularly effective in quenching or enhancing fluorescence emission of organic compounds, depending on the mutual distance between these and the gold surface [74, 75]. The corresponding dyes could be conjugated with gold nanoparticles due to adsorption process resulting in formation of non-covalent bond, covalent bond, and ionic interaction of positively charged groups with negatively charged surfaces of particles [76]. The main disadvantage of such hybrid systems is that the surface exposure of the dyes promotes their photooxidation. Another approach consists in the decoration of GNP dyes via bifunctional spacers, such as PEG or carboxylic acids, with subsequent chemical interaction of dyes with proper functional groups [53, 77].

The gold nanoparticles conjugated with dye molecules are very attractive because they can be studied by fluorescence-based techniques in addition to electron microscopy. If gold nanoparticles can successfully enhance the fluorescent signal of dyes to a significant degree, they would be useful in many areas of biochemistry and biology. For instance, dye-labeled gold particles could track the movements of drugs in cells and could act as a kind of molecular probe. Moreover, fluorescent-labeled gold nanoparticles are really highly selective imaging probes also because in contrast to scattering probes, their detection is not limited by the Rayleigh scattering conditions.

Besides direct effect on the transition strength, the reason to conjugate GNS with organic dyes is their successful application in SERS and fluorescence resonance energy transfer (FRET) assays. These application fields are discussed in Chaps. 2 and 3.

The GNS functionalized with dyes are schematically shown in Scheme 1.3.

Regarding fluorescence, quenching and energy transfer depend critically on the dye-gold distance. Navarro et al. reported in 2013 the synthesis, functionalization, and photophysics of luminescent hybrid gold nanostars prepared using a layer-by-layer

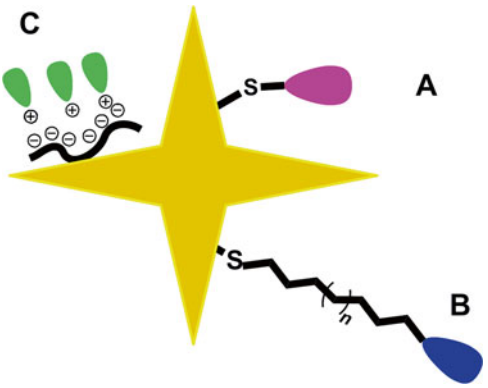

Scheme 1.3 Schematic representation of GNS functionalized with dyes via direct bounding (**A**), via bifunctional spacer (**B**), and through absorption onto surface (**C**)

(LbL) deposition method to tune the chromophore-to-particle distances, and studied the impact of the spectral overlap between the plasmon and the emission/absorption of the dyes on quenching [78]. Several luminescent dyes with different optical signatures were selectively adsorbed at the nanoparticle surface. The optimized systems, exhibiting the highest luminescence recovery, showed clearly that overlap must be as low as possible. The fluorescence intensities were quenched in close vicinity of the metal surface and revealed a distance dependence with almost full recovery of the emission when the dye was replaced by the 11 LbL layers, which corresponded to 15 nm distances evaluated on dried samples.

SERS-active probes were prepared by C. Khoury and Tuan Vo-Dinh by direct conjugation of p-mercaptobenzoic acid, a Raman-active dye, with synthesized GNS for potential use as SERS substrates in sensing [30]. In a more recent publication these authors presented a novel approach for the preparation of gold nanostar-functionalized substrates that show high sensitivity for chemical sensing based on surface-enhanced Raman spectroscopy [79]. Gold nanostars immobilized on a gold substrate via a Raman-silent organic tether serve as the SERS substrate, and facilitate the chemical sensing of analytes that can either be chemisorbed or physisorbed on the nanostars. For quantitative chemical detection based on SERS analysis, *p*-mercaptobenzoic acid is widely used as the model molecule. This is a Raman-active molecule with a relatively low-scattering cross section and *p*-mercaptobenzoic acid could be conjugated to GNS via its pendant thiol moiety as well as through π system interaction. In 2014 Khoury et al. presented also an effective method to distinguish intracellular from extracellular nanoparticles by selectively quenching the SERS signals from dye molecules absorbed onto star-shaped gold nanoparticles that have not been internalized by cells [80]. The conjugation of the fluorophores to the gold nanostars was achieved by first forming a cysteamine-Alexa 750 complex and then incubating it with PVP-capped GNS overnight. The dye-GNS conjugation efficiency was monitored through the observation of strong SERS signals from Alexa 750 at 789 nm [80].

An overview of recent developments and applications of surface-enhanced Raman scattering nanosensors has been published recently in *Nanomedicine and*

Nanobiotechnology [81]. The functionalization of GNS with different types of dyes and the properties of resulted systems were thoroughly discussed. For example, the functionalization of GNS with NAFTA6 dye, a derivative of 4-methoxy-1,8-naphthalimide bearing at the imide N-atom a long aliphatic chain with an SH terminal group, was reported [82]. In a second work, cyclic RGD peptide-modified GNS were subsequently labeled with a hydrophilic indocyanine green derivative (NIR fluorescent probe), to investigate the biodistribution of GNS and to assess the selective uptake of Au NS in tumors after attachment of cRGD [83]. The dye was activated with DCC and NHS before conjugation with cRGD-modified GNS. Vo-Dinh and coworkers reported in 2011 the synthesis and characterization of SERS label-tagged gold nanostars, coated with a silica shell containing methylene blue photosensitizing drug for singlet-oxygen generation [84]. The gold nanostars were tuned for maximal extinction in the NIR spectral region and tagged with an NIR dye (DTTC) for surface-enhanced resonance Raman scattering (SERRS). The use of an NIR dye further enhanced the SERS signal due to better spectral superposition. The protocol involving the silica coating was used by these authors to encapsulate the photosensitizer methylene blue in a shell around the nanoparticles as it is known that mesoporous silica shell can be used to encapsulate various dye molecules onto a metallic core. Methylene-blue-encapsulated nanoparticles showed a significant increase in singlet-oxygen generation as compared to nanoparticles synthesized without methylene blue.

In a different approach Melnikau et al. developed a hybrid system consisting of GNS and J-aggregates of the cyanine dyes and brought into evidence the coherent coupling between the localized plasmons of the metal component and the excitons of the J-aggregates through the Rabi splitting with the energy up to 260 meV [85]. J-aggregates were formed from the following two dyes: JC1 (5,5′,6,6′-tetrachloro-1,1′,3,3′-tetraethylimidacarbocyanine iodide) and S2165 2-[3-[1,1-dimethyl-3-(4-sulfobutyl)-1,3-dihydrobenzo[e]indol-2-ylidene]-propenyl]-1,1-dimethyl-3-(4-sulfobutyl)-1H-benzo[e] indolium hydroxide. Hybrid structures of gold nanostars and the J-aggregates of the JC1 dye were produced by the addition of the concentrated ethanol solution of the dye to an aqueous solution of gold nanostars in the presence of ammonia at pH 8. Interactions between nanostars and JC1 molecules of J-aggregates resulted in the formation of chain-like tightly bound agglomerates of gold nanostars interconnected by an organic matter.

It is worth noting that in 2009 a comparison study was published in which relevant photophysical properties of single-fluorescent molecules and single-SERS-active surface-coated gold nanostars tagged with the Raman reporter molecule 4-mercaptopyridine were compared for imaging purposes [86]. The nanostar-based SERS NP presented in this paper eliminates the traditional challenges of signal consistency and strength and demonstrates the viability of SERS probes for imaging applications. By comparing populations at the single-probe level, it was found that the count rate variance from a SERS NP is at least as good as that observed for fluorescent emission of Alexa Fluor 633. The preparation of gold nanostars modified with FITC-labeled chitosan was also reported later [87]. These modified GNS had a higher colloidal stability at physiological pH and they are more suitable mediators in cell photothermolysis due to the slower aggregation.

1.3.3 Other Examples of Functionalization of GNS

Functionalization of nanostructures GNS with biological molecules has many applications in biomedical imaging, clinical diagnosis, and therapy. A summary of the strategies of functionalization of GNS is shown in Scheme 1.4.

In most cases the functionalization of GNS aimed at the optimization of their intracellular delivery and photothermolysis efficiency. In order to increase the accumulation of nanoparticles at the tumor site and lower the side effects on normal tissues, many investigators have functionalized nanoparticles with ligands such as aptamer, peptide, and oligosaccharide for active tumor targeting. Moreover, besides the biological molecules, the functionalization of GNS with bifunctional spacers is also widely used for self-assembling monolayer formation and for further conjugation approaches.

The functionalization of gold nanoparticles, including GNS, with *peptides* is widely used. It was shown that *TAT-peptide*-functionalized gold nanostars enter cells significantly more than bare or PEGylated nanostars [88]. To fabricate stable constructs that resist aggregation in physiological environment and multiple washing

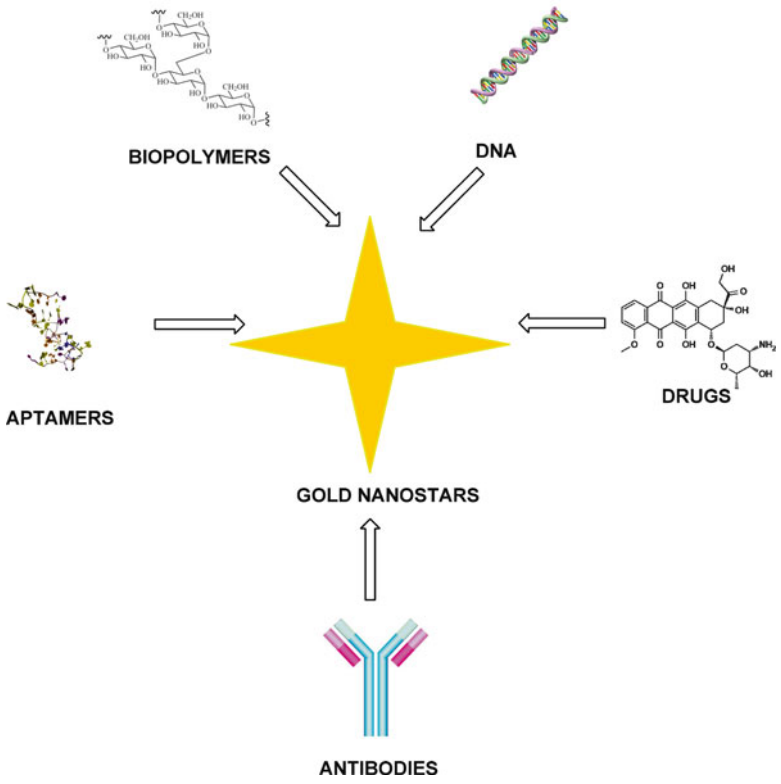

Scheme 1.4 General strategies of functionalization of GNS

cycles, GNS were decorated with cysteine-terminated TAT peptide and thiolated polyethylene glycol. The resulting constructs displayed enhanced intracellular delivery and efficient photothermolysis of TAT-modified nanostars and are considered promising agents in cancer therapy. *Biotin-functionalized* GNS were prepared by partial replacement of CTAB with biotinylated bovine serum albumin [89]. These functionalized GNS were used for detection of streptavidin. Nehl et al. bound mercaptohexadecanoic acid and *bovine serum* albumin to gold nanostars to create molecular sensors [38]. The observed shifts are consistent with the effects of these molecular layers on the surface plasmon resonances in continuous gold films. Vo-Dinh with coworkers presented the development of a theranostic system that combines Raman imaging and the photodynamic therapy effect [90]. The theranostic nanoplatform was created by loading the *photosensitizer*, *protoporphyrin IX*, onto a Raman-labeled gold nanostar. The co-decoration with a cell-penetrating peptide, TAT, enhanced intracellular accumulation of the nanoparticles and improved their delivery and efficacy. *TAT* conjugation was achieved by passive adsorption.

Aptamer-conjugated nanoparticles, especially gold nanoparticles, are promising for applications in bioanalysis and medical therapy, including early diagnosis and drug delivery. Novel valuable therapeutic complexes, namely *dual-aptamer*-modified gold nanostars, for the targeting of prostate cancers have been developed recently [60]. The aptamers were conjugated to PEGylated GNS via disulfide bonds. Nanoconstructs composed of nucleolin-specific aptamers and gold nanostars were actively transported to the nucleus and induced major changes to the nuclear phenotype via nuclear envelope invaginations near the site of the construct [91]. *AS1411 aptamers* containing thiol groups were grafted to GNS by capping molecule replacement, to create Apt–GNS nanoconstructs. To determine the number of aptamers attached to each GNS, the authors compared differences in fluorescence intensity of a solution of Cy5-labeled aptamer before and after conjugating the GNS. In an alternative application, highly selective, and reagent-free aptamer-based biosensor has been developed for quantitative detection of adenosine triphosphate [92]. The sensor contains a SERS probe made of gold nanostar-Raman label-SiO_2 core–shell nanoparticles in which the Raman label (malachite green isothiocyanate) molecules are sandwiched between a gold nanostar core and a thin silica shell [92]. The corresponding dye was chosen as the Raman label due to its nonfluorescent characteristic and its isothiocyanate (–N=*C*=S) group that can bind to the gold surface and is compatible with the SiO_2 encapsulation process as well. SiO_2 was employed as a protective layer because of its long-term stability and easy bioconjugation. These gold nanostars were finally functionalized with DNA. Firstly this process involved functionalization with 3-triethoxysilylpropyl succinic anhydride, and then the functionalization of DNA with carboxyl terminated constructs was carried out by the carbodiimide chemistry.

Dam et al. reported recently the design of a nanoconstruct that targets the ubiquitous protein nucleolin and that is largely independent of the cell phenotype [93]. Gold nanostars loaded with high densities of *nucleolin-specific DNA aptamer AS1411* produced anticancer effects in a panel of 12 cancer lines containing four representative subcategories. Thiolated AS1411 was attached to the AuNS surface via gold–sulfur

bonds in a 2-day "salt-aging" process. It was found that high loading densities of Apt on the AuNS increased the overall stability of aptamers in physiological environments, similar to other reports of nucleic acids on spherical gold particles.

The conjugation of *antibodies and RNA moieties* to gold nanoparticles is also widely used in a range of approaches. Liz-Marzan et al. developed an inverse sensitivity assay based on the detection of the plasmon resonance shift induced by the growth of silver crystals on the gold nanostars [94]. To control crystal growth the authors used the enzyme glucose oxidase (GOx), which generates hydrogen peroxide that reduces silver ions. Only when the enzyme is present at low concentration the reducing agent is in short supply and the crystal growth is slow, favoring the formation of a homogeneous silver coating on the gold nanostars with respect to single-silver nanocrystals. Once proved this inverse sensitivity mechanism, the GNS were modified with polyclonal antibodies against prostate-specific (rabbit) antigen and used as the label in a classical enzyme-linked immunoassay. This mechanism was demonstrated on polyclonal anti-PSA (rabbit) antibody.

Wege et al. described an RNA-directed bottom-up assembly procedure yielding bioinorganic hybrid nanostars with a central gold core and a surface-saturating number of virus-derived arms. These constructs are not gold nanostars but branched gold-based organic nano-objects with an exceptionally high and tunable ratio of the virus-based surface arms to the metal cores [95]. This was achieved by binding on the gold beads short oligonucleotides complementary for the initial sequence of the tobacco mosaic virus (TMV) *RNA*. The TMV RNA triggers the formation of the virus coat protein assembly in the peculiar rodlike shape of the TMV. The specificity of RNA hybridization to oligo-deoxynucleotides exposed on gold nanoparticles of different diameters allowed the simultaneous fabrication of star colloids with distinct predetermined arm-length distributions in single-batch processes [95].

Surface functionalization of GNS with ethylene glycol-modified Raman reporter derivatives Ra_1 and Ra_2 was adopted for both hydrophilic stabilization and subsequent biofunctionalization [96]. The two organic compounds Ra_1 and Ra_2 were synthesized from the Raman reporter molecule 5,5′-dithiobis(2-nitrobenzoic acid) by the formation of the corresponding amides with a short hydrophilic monoethylene glycol spacer (H_2N–MEG–OH for Ra_1) and a longer hydrophilic triethylene glycol spacer (H_2N–TEG–COOH for Ra_2), respectively. Bioconjugation of the SERS label to the anti-p63 antibody was achieved via activation of the COOH groups in Ra_2 using standard EDC/s-NHS chemistry.

In the paper published in 2009 a dynamic mode of optical contrast based on gyromagnetic imaging, in which gold nanostars with superparamagnetic cores are driven by a rotating magnetic field gradient to produce periodic variations in NIR scattering intensities, was presented [97]. These GNS were functionalized with oligoethyleneglycol-conjugated folic acid derivatives by in situ dithiocarbamate formation, followed by membrane dialysis.

For many purposes the functionalization with several species is also widely used. For example in previously cited paper gold nanostars were conjugated with *cyclic RGD* and NIR fluorescence probe or *anticancer drug* (*DOX*) to obtain multifunctional nanoconstructs [82]. Using tumor cells and tumor-bearing mice, these imaging nanoparticles demonstrated favorable tumor-targeting capability mediated by RGD

peptide binding to its over-expressed receptor on the tumor cells. The nanostars functionalized with RGD and DOX integrated targeting tumor, chemotherapy, and photo-thermotherapy into a single system. The synergistic effect of photothermal therapy and chemotherapy was demonstrated in different tumor cell lines and in vivo using S180 tumor-bearing mouse models. Gold nanostars have been assembled via electrostatically assisted *3-aminopropyltriethoxysilane* (APTES)-functionalized surface assembly method [98] to produce a substrate with SERS activity. The most attractive advantage of electrostatically assisted APTES-functionalized surface assembly method is that a substrate with a very homogeneous SERS signal and large area can be fabricated without sophisticated equipment. Plasmonic gold nanostars were also modified with a biopolymer *chitosan* [87]. The chitosan-modified nanostars dispersed in a medium with pH = 7.5 had higher stability than those of chitosan-capped nanorods because of the slower aggregation of GNS. At pH = 7.5 the chitosan-modified GNS formed aggregates with highly nonuniform sizes.

Wei et al. presented in 2012 a new surface-enhanced Raman spectroscopy platform suitable for gas-phase sensing based on the extended organization of *poly-N-isopropylacrylamide* (pNIPAM)-coated nanostars over large areas [99]. The authors reported the preparation of optically active gold nanostars coated with pNIPAM and their controlled assembly into highly ordered linear structures. Au-pNIPAM core–shell particles were prepared by precipitation polymerization of the monomer NIPAM in the presence of functionalized, spherical gold nanoparticles. pNIPAM-coated gold nanoparticles were dispersed in solution with PVP, and the solution was incubated overnight to allow diffusion of PVP to the Au surface. Nanostars were formed by adding to the resulted solution an aqueous solution of $HAuCl_4$.

A highly sensitive SERS-based sandwich immunoassay employed two derivatives of gold nanostars simultaneously [100]. One was densely packed self-assembled substrates of gold nanostars and the other was made of immune-labeled nanostar aggregates. 4-Mercaptobenzoic acid-labeled immune-labeled gold nanostar aggregates were obtained by successive Raman reporter replacement, aggregation, immune immobilization, and blocking. Gold nanostar multilayers were formed by the self-assembly between polyelectrolytes and gold nanostars through electrostatic interaction.

The GNS could also be decorated with mixed *lipid-polymer* coatings by exploiting thiol chemistry [101]. This multiple decoration would increase/modify their interaction with skin and enable the nanoparticles' drug delivery capabilities. Polymers capable of trapping and releasing drugs under temperature control obtained by NIR laser irradiation may in fact be employed for this purpose.

The integration of metal nanoparticles within cross-linked polymeric microgels, in a well-defined core–shell structure, offers unique possibilities in various fields due to the potential to introduce multiple functionalities by tailoring the properties of the inorganic and the organic components [102]. Recently the encapsulation of gold nanoparticles within pNIPAM (poly-*N*-isopropylacrylamide) microgels has been reported for different particle sizes, including nanostars. All strategies start from initial modification of the metallic surface with molecules containing vinyl groups, which serve as starting points for the polymerization and thus facilitate the

encapsulation. The resulted colloidal nanocomposites based on a metallic core and a pNIPAM shell preserve the main properties of both components, i.e., the optical response from the plasmonic nanoparticle and the thermosensitive behavior of the polymer shell [102]. The synthesis and application of such composites are described in an interesting highlight of Liz-Marzan et al. [103].

Esentruk and Walker produced *iron oxide-coated* gold nanostars by first synthesizing gold nanostars (ca 150 nm), and then introducing a PVP coating followed by reducing iron(II) and iron(III) salts on the nanoparticle (NP) surface [104]. Having both magnetic and plasmonic properties in one NP system makes these particles suitable for various bio-analytical applications such as biomolecule separation, sensing, and magnetic imaging.

A novel synthetic methodology for star-shaped *gold-coated magnetic* nanoparticles was reported in a paper published in 2014 in RCS Adv [105]. The coating was performed in two steps: formation of gold nuclei at the surface of magnetite nanoparticles followed by growth of the gold nuclei into a complete star-shaped shell. The star-shaped gold-coated magnetic nanoparticles thus obtained preserve the magnetic properties of the precursor magnetite nanoparticles; for example they can be easily separated with a magnet. In addition, the gold coating provides interesting optical properties while simultaneously allowing for biofunctionalization that may be advantageous for biological applications, such as (bio)detection via SERS. As a proof of concept, the GNS were modified with a capping agent terminated with a nickel(II)-nitrilotriacetate group that shows high affinity for histidine. The resulting star-shaped nanoparticles were used to selectively capture histidine-tagged maltose-binding protein from a crude cell extract. The performance of star-shaped gold-coated magnetic nanoparticles as SERS platforms was demonstrated through the detection of Raman-active dye (Astra Blue).

It has been already mentioned that a mesoporous *silica shell* can be used to encapsulate various dye molecules onto a metallic core. Vo-Dinh and coworkers developed and characterized label-tagged gold nanostars, coated with a silica shell containing methylene blue [84]. Silica encapsulation on GNS and their intracellular SERS detection were also reported by the same research group [106].

Gold nanostars due to a range of properties are promising platforms for applications in medicine and biology. The techniques used for their synthesis were reviewed in this chapter. Since for a variety of applications surface functionalization of GNS is essential, different functionalization approaches were also discussed here. The next chapter focuses on physical properties giving an explanation of righteous reinforced attention to these types of gold nanoparticles.

References

1. Zhou J, Ralston J, Sedev R, Beattie DA (2009) Functionalized gold nanoparticles: synthesis, structure and colloid stability. J Colloid Interface Sci 331:251–262
2. Frens G (1971) Controlled nucleation for the regulation of the particle size in monodisperse gold suspension. Nat Phys Sci 241:20–22

3. Hostetler M et al (1998) Alkanethiolate gold cluster molecules with core diameters from 1.5 to 5.2 nm: core and monolayer properties as a function of core size. Langmuir 14:17–30
4. Zhao P, Li N, Astruc D (2013) State of the art in gold nanoparticle synthesis. Coord Chem Rev 257:638–665
5. Turkevich J, Stevenson PC, Hillier J (1951) A study of the nucleation and growth process in the synthesis of colloidal gold. Discuss Faraday Soc 11:55–75
6. Kimling J et al (2006) Turkevich method for gold nanoparticle synthesis revisited. J Phys Chem 110:15700–15707
7. Pong BK et al (2007) New insights on the nanoparticles growth mechanism in the citrate reduction of gold (III) salt: formation of the Au nanowire intermediate and its nonlinear optical properties. J Phys Chem 111:6281–6287
8. Polte J et al (2010) Mechanism of gold nanoparticle formation in the classical citrate synthesis method derived from coupled in situ XANES and SAXS evaluation. J Am Chem Soc 132:1296–1301
9. Kumar S, Gandhi KS, Kumar R (2007) Modeling of formation of gold nanoparticles by citrate method. Ind Eng Chem Res 46:3128–3136
10. Brust M et al (1994) Synthesis of thiol-derivatised gold nanoparticles in a two-phase liquid-liquid system. J Chem Soc Chem Commun 7:801–802
11. Brust M et al (1995) Synthesis and reactions of functionalized gold nanoparticles. J Chem Soc Chem Commun 16:1655–1656
12. Templeton AC, Wuelfing WP, Murray WP (2000) Monolayer-protected cluster molecules. Acc Chem Res 33:27–36
13. Sardar R, Shumaker-Parry JS (2009) 9-BBN induced synthesis of nearly monodispersed ω-functionalized alkylthiol stabilized gold nanoparticles. Chem Mater 21:1167–1169
14. Mallick K, Wang ZL, Pal T (2001) Seed-mediated successive growth of gold particles accomplished by UV irradiation: a photothermal approach of size-controlled synthesis. J Photochem Photobiol A 140:75–80
15. Kumar SP et al (2008) High-yield synthesis and optical response of gold nanostars. Nanotechnology 19:015606
16. Burda C et al (2005) Chemistry and properties of nanocrystals of different shapes. Chem Rev 105:1025–1102
17. Casu A, Cabrini E et al (2012) Controlled synthesis of gold nanostars by using zwitterionic surfactant. Chemistry 18:9381–9390
18. Guerro-Martinez A et al (2011) Nanostars shine bright to you: colloidal synthesis, properties and application of branched metallic nanoparticles. Curr Opin Colloid Interface Sci 16:118–127
19. Alvarez-Puebla R, Liz-Marzan LM, Garcia De Abajo FJ (2010) Light concentration at the nanometer scale. J Phys Chem Lett 1:2428–2434
20. Freddi S, Sironi L et al (2013) A molecular thermometer for nanoparticles for optical hyperthermia. Nano Lett 13:2004–2010
21. Hrelesku C et al (2009) Single gold nanostars enhance Raman scattering. Appl Phys Lett 94:1–3
22. Gasser U, Weeks ER, Schofield A, Pusey PN, Weitz DA (2001) Real-space imaging of nucleation and growth in colloidal crystallization. Science 292:258–262
23. Kawamura G, Nogami M (2009) Application of a conproportionation reaction to a synthesis of shape-controlled gold nanoparticles. J Cryst Growth 311:4462–4466
24. Sau TK, Murphy CJ (2004) Room temperature, high-yield synthesis of multiply shapes of gold nanoparticles in aqueous solution. J Am Chem Soc 126:8648–8649
25. Kuo CH, Huang MH (2005) Synthesis of branched of gold nanocrystals by a seeding growth approach. Langmuir 21:2012–2016
26. Wu HL, Chen CH, Huang M (2009) Seed-mediated of branched gold nanocrystals derived from the side growth of pentagonal bipyramids and the formation of gold nanostars. Chem Mater 21:110–114
27. Zou H, Ying E, Dong S (2006) Seed-mediated synthesis of branched gold nanoparticles with the assistance of citrate and their surface-enhanced Raman scattering properties. Nanotechnology 17:4758–4764

28. Barbosa S et al (2010) Size tuning and sensing capabilities of gold nanostars. Langmuir 26:14943–14950
29. Minati L et al (2014) One-step synthesis of star-shaped gold nanoparticles. Colloids Surf A Physicochem Eng Asp 441:623–628
30. Khoury CG, Vo-Dinh T (2008) Gold nanostars for surface-enhanced Raman scattering: synthesis, characterization and optimization. J Phys Chem C 112:18849–18859
31. Yuan H, Khoury CG et al (2012) Gold nanostars: surfactant-free synthesis, 3D modelling, and two-photon photoluminescence imaging. Nanotechnology 23:075102
32. Osinkina L et al (2013) Synthesis of gold nanostar arrays as reliable, large-scale homogeneous substrates for surface-enhanced Raman scattering imaging and spectroscopy. J Phys Chem C 117(43):22198–22202
33. Li Y, Ma J, Ma Z (2013) Synthesis of gold nanostars with tunable morphology and their electrochemical application for hydrogen peroxide sensing. Electrochim Acta 108:435–440
34. Chirea M (2013) Electron transfer of gold nanostars assemblies: a study of shape stability and surface density influence. Catalysts 3:288–309
35. Kereselidze Z, Romero VH, Peralta XG, Santamaria F (2012) Gold nanostar synthesis with a silver seed mediated growth method. JoVE Bioeng. doi:10.3791/3570
36. Salinas K et al (2014) Transient extracellular application of gold nanostars increases hippocampal neuronal activity. J Nanobiotechnol 12:31
37. Stassi S et al (2012) Synthesis and characterization of gold nanostars as filler of tunneling conductive polymer composites. Eur J Inorgan Chem 16:2669–2673
38. Pallavicini P, Dona A et al (2013) Triton X-100 for three-plasmon gold nanostars with two photothermally active NIR (near IR) and SWIR (short-wavelength IR) channels. Chem Commun 49:6265–6267
39. Nehl CL, Liao H, Hafner JH (2006) Plasmon resonant molecular sensing with single gold nanostars. Proc SPIE 6323:63230G
40. Sau TK, Rogach AL, Döblinger M, Feldmann J (2011) One-step high-yield aqueous synthesis of size-tunable multispiked gold nanoparticles. Small 7:2188–2194
41. Xia Y, Xiong Y, Lim B, Skrabalak SE (2009) Shape-controlled synthesis of metal nanocrystals: simple chemistry meets complex physics? Angew Chem Int Ed 48:60–103
42. Xie J, Lee JY, Wang DIC (2007) Seedless, surfactantless, high-yield synthesis of branched nanocrystals in HEPES buffer solution. Chem Mater 19:2823–2839
43. Jena BK, Raj CR (2007) Synthesis of flower-like gold nanoparticles and their electrocatalytic activity towards oxidation of methanol and the reduction of oxygen. Langmuir 23: 4064–4070
44. Yamamoto M, Kashiwagi Y, Sakata T, Mori H, Nakamoto M (2005) Synthesis and morphology of star-shaped gold nanoplates protected by Poly(N-vinyl-2-pyrrolidone). Chem Mater 17:5391–5393
45. Hao E, Bailey RC, Scharz GC, Hupp JT, Li S (2004) Synthesis and optical properties of "branched" gold nanocrystals. Nano Lett 4:327–330
46. Umedevi S, Lee HC, Ganesh V, Feng X, Hegmann T (2014) A versatile, one-pot synthesis f gold nanostars with long, well-defined, thorns using a lyotropic liquid crystal template. Liquid Crystals 41:265–276
47. Moukarzel W, Fitremann J, Marty JD (2011) Seed-less amino-sugar-mediated synthesis of gold nanostars. Nanoscale 8:3285–3290
48. Zhou M, Chen S, Zhao S (2006) Preparation of branched gold nanocrystals by an electrochemical method. Chem Lett 35:332–333
49. Li Z, Li W, Camargo PHC, Xia Y (2008) Facile synthesis of branched Au nanostructures by templating against a self-destructive lattice of magnetic Fe nanoparticles. Angew Chem Int Ed 47:9653–9656
50. Chirumamilla M et al (2014) Plasmon resonance tuning in metal nanostars for surface enhanced Raman scattering. Nanotechnology 25:235303
51. Chirumamilla M et al (2014) 3D nanostars dimers with a sub-10-nm gap for single-/few-molecule surface enhanced Raman scattering. Adv Mater 26:2353–2358

52. Park G, Seo D, Chung IS, Song H (2013) Poly(ethylene glycol)- and carboxylate-functionalized gold nanoparticles using polymer linkages: single-step synthesis, high stability, and plasmonic detections of proteins. Langmuir 29:13518–13526
53. Tiwari PM et al (2011) Functionalized gold nanoparticles and their biomedical applications. Nanomaterials 1:31–63
54. Sperling RA, Parak WJ (2010) Surface modification, functionalization and bioconjugation of colloidal inorganic nanoparticles. Phil Trans R Soc A 368:1333–1383
55. Rahme K et al (2013) PEGylated gold nanoparticles: polymer quantification as a function of PEG lengths and nanoparticles dimensions. RSC Adv 3:6085–6095
56. Sanna V, Pala N, Sechi M (2014) Targeted therapy using nanotechnology: focus on cancer. Int J Nanomed 9:467–483
57. Kumar R et al (2013) Third generation gold nanoplatform optimized for radiation therapy. Transl Cancer Res 4:228–239
58. Manson J, Kumar D, Meenan BJ, Dixon D (2011) Polyethylene glycol functionalized gold nanoparticles: the influence of capping density on stability in various media. Gold Bull 44:99–105
59. Navarro JR et al (2012) Synthesis of PEGylated gold nanostars and bipyramids for intracellular uptake. Nanotechnology 46:465602
60. Jo H et al (2014) Ultra-effective photothermal therapy for prostate cancer cells using dual-aptamer modified gold nanostars. J Mater Chem B 2:4862–4867
61. Yuan H et al (2012) In vivo particle tracking and photothermal ablation using plasmon-resonant gold nanostars. Nanomed Nanotechnol Biol Med 8:1355–1363
62. Cennamo N et al (2013) Localized surface plasmon resonance with five branched gold nanostars in a plastic optical fiber for bio-chemical sensor implementation. Sensors (Basel) 13:14676–14686
63. Wang S et al (2013) Single continuous wave laser induced photodynamic/plasmonic photothermal therapy photosensitizer-functionalized gold nanostars. Adv Mater 25:3055–3061
64. Li W et al (2014) *In vivo* quantitative photoacoustic microscopy of gold nanostars kinetics in mouse organs. Biomed Opt Express 5(8):2679–2685. doi:10.1364/BOE.5.002679
65. Chen X, Wong STC (eds) (2014) Cancer theranostic. Academic, London
66. Nune SK et al (2009) Nanoparticles for biomedical imaging. Expert Opin Drug Deliv 6:1175–1194
67. Song Y, Zhu S, Yang B (2014) Bioimaging based on fluorescent carbon dots. RSC Adv 4:27184–27200
68. Zedler L et al (2012) Ruthenium dye functionalized gold nanoparticles and their spectral responses. RSC Adv 2:4463–4471
69. Narband N et al (2009) The interaction between gold nanoparticles and cationic and anionic dyes: enhanced UV-visible absorption. Phys Chem Chem Phys 44:10513–10518
70. Sironi L et al (2009) p53 Detection by fluorescence lifetime on a hybrid fluorescein isothiocyanate gold nanosensor. J Biomed Nanotechnol 5:683–691
71. Cordes DB et al (2005) Optical glucose detection across the visible spectrum using anionic fluorescent dyes and a viologen quencher in a two-component saccharide sensing system. Org Biomol Chem 3:1708–1713
72. Leung CH et al (2012) Luminescent detection of DNA-binding proteins. Nucleic Acids Res 40:941–955
73. Radwan SH, Azzazy HME (2009) Gold nanoparticles for molecular diagnostic. Expert Rev Mol Diagn 9:511–524
74. Yang PJ et al (2012) Quenching effects of gold nanoparticles in nanocomposites formed in water-soluble conjugated polymer nanoreactors. Polymer 53:239–946
75. Dulkeith E et al (2005) Gold nanoparticles quench fluorescence by phase induced radiative rate suppression. Nano Lett 5:585–589
76. Hutter E, Maysinger D (2013) Trends Pharmacol Sci 34:497–506
77. Conde J et al (2014) Revisiting 30 years of biofunctionalization and surface chemistry of inorganic nanoparticles for nanomedicine. Front Chem 2:48

78. Navarro JRG et al (2013) Tuning dye-to-particle interactions toward luminescent gold nanostars. Langmuir 29:10915–10921
79. Indrasekara AS et al (2014) Gold nanostar substrates for SERS-based chemical sensing in the femtomolar regime. Nanoscale 6:8891–8899
80. Xie N, Lin Y, Mazo M, Chiappini C et al (2014) Identification of intracellular gold nanoparticles using surface-enhanced Raman scattering. Nanoscale 6:12403–12407
81. Vo-Dinh T et al (2014) SERS nanosensors and nanoreporters: golden opportunities in biomedical application. Nanomed Nanobiotechnol. doi:10.1002/wnan.1283
82. Giorgetti E et al (2012) Tunable gold nanostars for surface enhanced Raman spectroscopy. Phys Stat Solidi B 249:1188–1192
83. Chen H et al (2013) Multifunctional gold nanostar conjugates for tumor imaging and combined photothermal and chemo-therapy. Theranostics 3:633–649
84. Fales AM, Yuan H, Vo-Dinh T (2011) Silica-coated gold nanostars for combined surface-enhanced Raman scattering (SERS) detection and singlet-oxygen generation: a potential nanoplatforms for theranostics. Langmuir 27:12186–12190
85. Melnikau D et al (2013) Strong plasmon-exciton coupling in a hybrid system of gold nanostars and J-aggregates. Nanoscale Res Lett 8:134
86. Allegeyer ES et al (2009) Optical signal comparison of single fluorescent molecules and Raman active gold nanostars. Nano Lett 9:3816–3819
87. Baginskiy I et al (2013) Chitosan-modified stable colloidal gold nanostars for the thermolysis of cancer cells. J Phys Chem 117:2396–2410
88. Yuan H et al (2012) TAT-peptide functionalized gold nanostars: enhanced intracellular delivery and efficient NIR photothermal therapy using ultralow irradiance. J Am Chem Soc 134: 11358–11361
89. Dondapati S et al (2010) Label-free biosensing based on single gold nanostars as plasmonic transducers. ACS Nano 4:6318–6322
90. Fales AM, Yuan H, Vo-Dinh T (2013) Cell-penetrating peptide enhanced intracellular Raman imaging and photodynamic therapy. Mol Pharm 10:2291–2298
91. Dam DH et al (2012) Direct observation of nanoparticles-cancer cell nucleus interactions. ACS Nano 6:3318–3326
92. Li M et al (2012) Detection of adenosine triphosphate with an aptamer biosensor based on surface-enhanced Raman scattering. Anal Chem 84:2837–2842
93. Dam DHM et al (2014) Grafting aptamers onto gold nanostars increases in vitro efficacy in a wide range of cancer cell types. Mol Pharm 11:580–587
94. Rodriguez-Lorenzo L et al (2012) Plasmonic nanosensors with inverse sensitivity by means of enzyme-guided crystal growth. Nat Mater 11:604–607
95. Eber FJ et al (2013) Bottom-up-assembled nanostar colloids of gold cores and tubes derived from tobacco mosaic virus. Angew Chem 125:7344–7348
96. Schutz M et al (2011) Hydrophilically stabilized gold nanostars as SERS labels for tissue imaging of the tumor suppressor p63 by immuno-SERS microscopy. Chem Commun 47:4216–4218
97. Wei Q et al (2009) Gyromagnetic imaging: dynamic optical contrast using gold nanostars with magnetic core. J Am Chem Soc 131:9728–9734
98. Su Q et al (2011) A reproducible SERS substrate based on electrostatically assisted APTES-functionalized surface-assembly of gold nanostars. ACS Appl Mater Interface 3:1873–1879
99. Mueller M et al (2012) Large-area organization of pNIPAM-coated nanostars as SERS platforms for polycyclic aromatic hydrocarbons sensing in gas phase. Langmuir 28:9168–9173
100. Pei Y et al (2013) Highly-sensitive SERS-based immunoassay with simultaneous utilization of self-assembled substrates of gold-nanostars and aggregates of gold nanostars. J Mater Chem B 1:3992–3998
101. Chirico G, Pallavicini P, Collini M (2014) Gold nanostars for superficial diseases: a promising tool for localized hyperthermia? Nanomedicine 9:1–3
102. Perez-Juste J, Pastoriza-Santos I, Liz-Marzan LM (2013) Multifunctionality in metal@microgel colloidal composites. J Mater Chem A 1:20–26

103. Caceres-Contreras R et al (2008) Encapsulation and growth of gold nanoparticles in thermo-responsive microgels. Adv Mater 20:1666–1670
104. Esentruk EN, Walker AR (2013) Gold nanosrars@iron oxide core-shell nanostructures: synthesis, characterization, and demonstrated surface-enhanced Raman scattering properties. J Nanopart Res 15:1364
105. Quaresma P et al (2014) Star-shaped magnetic@gold nanoparticles for protein magnetic separation and SERS detection. RSC Adv 4:3659–3667
106. Yuan H et al (2012) Spectral characterization and intracellular detection od surface-enhanced Raman scattering (SERS)-encoded plasmonic gold nanostars. J Raman Spectrosc 44:234–239